

Clover - Measuring the cosmic microwave background B-mode polarization

P. K. Grimes⁴, P. A. R. Ade¹, M. D. Audley², C. Baines³, R. A. Battye³, M. L. Brown², P. Cabella⁴, P. G. Calisse¹, A. D. Challinor^{5,6}, P. J. Diamond³, W. D. Duncan⁷, P. Ferreira⁴, W. K. Gear¹, D. Glowacka², D. J. Goldie², W. F. Grainger¹, M. Halpern⁸, P. Hargrave¹, V. Haynes³, G. C. Hilton⁷, K. D. Irwin⁷, B. R. Johnson⁴, M. E. Jones⁴, A. N. Lasenby², P. J. Leahy³, J. Leech⁴, S. Lewis³, B. Maffei³, L. Martinis³, P. Maudkopf¹, S. J. Melhuish³, C. E. North^{1,4}, D. O’Dea², S. M. Parsley¹, L. Piccirillo³, G. Pisano³, C. D. Reintsema⁷, G. Savini¹, R. Sudiwala¹, D. Sutton⁴, A. C. Taylor⁴, G. Teleberg¹, D. Titterton², V. Tsaneva², C. Tucker¹, R. Watson³, S. Withington², G. Yassin⁴, J. Zhang¹ and J. Zuntz⁴.

Abstract—Clover is a UK-led experiment to measure the B-mode polarization of the cosmic microwave background. The instruments are currently under construction and deployment to the Pampa La Bola site in the Atacama Desert is planned for 2010. It consists of two 2-m class telescopes feeding background limited imaging arrays of ~100 dual polarization pixels at each of 97, 150 and 225 GHz. The waveguide and antenna fed TES bolometers are limited by unavoidable photon noise from the atmosphere, and read-out using NIST’s time domain multiplexing scheme. The entire instrument has been designed for exceptionally low systematic errors in polarization measurements, which has necessitated novel designs for the instrument optics, horn arrays, OMTs and detector feeds, as well as careful development of the scan strategy, field location and data analysis methods.

The experiment aims to measure the polarization of the CMB with an angular resolution of $5.5' - 8'$ across 1000 deg^2 of sky (angular multipole range $20 < l < 1000$) to a sensitivity of $8 \mu\text{K-arcmin}$ after foreground cleaning. If all systematics are adequately controlled this will allow the detection of the primordial B-mode CMB anisotropies down to tensor to scalar ratios of 0.03, as well as providing extremely accurate measurements of the CMB temperature, E-mode polarization, and B-mode lensing polarization. Detecting or constraining the level of the primordial B-mode signal will allow constraints to be placed on the energy scale of inflation, providing an unprecedented insight into the physics of the early Universe.

We describe the current status of the Clover project, including the current instrument design and construction status, and the development of the novel technology involved.

Index Terms—Cosmic Microwave Background, B-mode polarization, ground-based telescope, cosmology

I. INTRODUCTION

PRECISE measurements of the polarization of the cosmic microwave background (CMB) can provide constraints on a number of cosmological parameters, possibly including the

energy scale of inflation. A measurement of the energy scale of inflation would tell us about the physics of the Big Bang itself for the first time [1].

CMB polarization fluctuations are usually decomposed into two orthogonal modes; a “grad-like” E-mode with electric field-like parity, and a “curl-like” B-mode with magnetic field-like parity [2]. Primordial density perturbations in the early universe give rise to both the large scale distribution of matter in the universe and to the CMB intensity anisotropies. These density perturbations also generate the purely E-mode polarization fluctuations, or “E-modes” at about 10% of the intensity fluctuations (rms level $\sim 5 \mu\text{K}$).

Magnetic field-like polarization fluctuations, or “B-modes” are not generated directly by primordial density perturbations. B-modes can be either generated by gravitational lensing of the primordial CMB intensity and E-mode polarization fluctuations by matter after decoupling of the CMB (the “B-mode lensing signal”), or by tensor fluctuations at the surface of last scattering, caused by primordial gravity waves. These primordial B-modes are a key diagnostic of inflationary cosmology theories, with the intensity of the gravity wave fluctuations giving a key insight to the energy scale and form of the inflationary field. As such, the CMB primordial B-mode signal provides a key insight into the physics of the very early universe, allowing us to probe physics at energy scales around 10^{16} GeV .

Based on the current ΛCDM concordance cosmology model, the primordial B-mode signal is expected to be at least 10-100 times weaker than the E-mode signal. Therefore its detection and characterization will require novel dedicated experiments with at least 1-2 orders of magnitude more sensitivity than current CMB polarization experiments.

A. The Clover project

Clover is a UK-led project that aims to measure the primordial B-mode CMB signal, or to constrain its level to a tensor-to-scalar fluctuation ratio $r < 0.026$ in an angular multipole range of $20 < l < 1000$ ($8'$ to 10°). This is a factor of 10 lower than the current limits, and would confirm or rule out a number of theories of inflation.

¹School of Physics and Astronomy, Cardiff University, UK.

²Cavendish Laboratory, University of Cambridge, UK.

³School of Physics and Astronomy, University of Manchester, UK.

⁴Astrophysics, Dept. of Physics, University of Oxford, UK.

⁵Institute of Astronomy, University of Cambridge, UK.

⁶DAMTP, University of Cambridge, UK.

⁷National Institute of Standards and Technology, USA.

⁸University of British Columbia, Canada.

P. Cabella is now with the University of Rome, Italy.

B.R. Johnson is now with the University of California, Berkeley, USA

Clover will spend two years making polarimetric observations of approximately 1000 square degrees of the sky from Pampa la Bola on the ALMA site in the Atacama Desert, Chile. Clover consists of two ~ 2 m Compact Range Antenna telescopes feeding imaging arrays of 96 dual polarized antenna-coupled Transition Edge Sensor (TES) bolometers at each of 97, 150 and 225 GHz. The Clover instruments use a number of techniques, including rapid constant elevation scanning, polarization modulation via half-wave plates, and absorbing ground shields to reduce systematic errors.

The two Clover telescopes are currently being assembled by the Astrophysics group at the University of Oxford, with the receivers undergoing cryogenic tests in the Astronomical Instrumentation Group at Cardiff University. The science grade detectors are currently being fabricated at the Detector Physics Group, Cavendish Laboratories, Cambridge and the 97 GHz array feed-horns and OMTs are being tested at University of Manchester. The two Clover instruments will then be integrated and tested at Oxford, before shipping to Chile for installation and commissioning.

B. Ancillary Science Goals

Clover will also make precise measurements of the CMB intensity and E-mode signals, and will measure the non-primordial B-mode lensing signal. These measurements will provide tighter constraints on cosmological parameters and will complement measurements made by Planck and other instruments. Clover will also be sensitive to a number of effects due to exotic physics in the early universe, particularly parity violation which results in correlations between the CMB intensity and E-mode signals and the B-mode signal, and B-mode signal from a background population of topological defects such as cosmic strings.

II. INSTRUMENT DESCRIPTION

A. Instrument requirements

The ambitious science goals of Clover mean that the requirements on both sensitivity and control of systematic errors are extremely stringent [3]. Some of the major requirements are listed in Table I.

Characterizing the B-mode fluctuation power spectrum for a tensor-to-scalar ratio of $r = 0.026$ requires mapping a sky area of ~ 1000 deg² to an rms noise of $1.4 \mu\text{K}$ per $5.5'$ pixel for the 150 GHz instrument. To reach the overall sensitivity across the survey areas in a reasonable integration time, the system noise must be comparable or lower than the unavoidable photon noise from the atmospheric and astronomical background. This results in stringent requirements on the detector noise, the instrument efficiency and on spillover from the optics.

Separating the CMB polarization signal from the strongest polarized astrophysical foreground signals (dust [4] and galactic synchrotron radiation [5]), requires that observations are made at three or more frequency bands across the expected foreground minimum at ~ 100 GHz. The chosen Clover band-passes and the expected atmospheric photon noise and transparency are shown in Table II.

Table I
SUMMARY OF REQUIREMENTS ON THE CLOVER INSTRUMENTS

Instrument Characteristic	Requirement
Stokes parameters measured	I, Q and U at each pixel
Multipole range	$20 < l < 1000$
Resolution	$8'$
Mapped area	1000 deg^2
RMS Noise per $5.5'$ map pixel (Q, U)	$1.4 \mu\text{K}$
Instrument noise limit	Unavoidable photon noise
Detector NET (97, 150, 225 GHz)	$150, 225, 590 \mu\text{K}\sqrt{\text{Hz}}$
Detector NEP (97, 150, 225 GHz)	$2, 4, 8 \times 10^{-17} \text{ W}/\sqrt{\text{Hz}}$
# FPA pixels (97, 150, 225 GHz)	96, 96, 96
Field of view (97, 150, 225 GHz)	$4.10^\circ, 3.42^\circ, 4.81^\circ$
Residual $Q \longleftrightarrow U$ rotation (Cross-pol)	$0.24^\circ (< 1.4\%)$
Q, U loss (depolarization)	$< 10\%$
Residual $T \longleftrightarrow Q, U$ mixing	$< 0.015\%$
Polarization beam misalignment	$< 0.2\% \text{ FWHM}$
Beam ellipticity	< 0.85
Differential beam ellipticity	< 0.012
Polarization modulation efficiency	$> 90\%$
Absolute calibration	$< 5\%$

Table II
CLOVER OBSERVING BANDS. MEAN τ AND NEP_{sky} ARE CALCULATED AT THE ZENITH FOR A 50% QUANTILE ATMOSPHERE [6].

Band Pass	Mean τ	$NEP_{sky} (\times 10^{-17} \text{ W}/\sqrt{\text{Hz}})$
82 – 112 GHz	0.014	1.67
125 – 175 GHz	0.023	3.08
192 – 258 GHz	0.047	5.43

In order to prevent instrumental polarization of the CMB intensity fluctuations from swamping the B-mode polarization signal, the instrumental (de-)polarization (Stokes's I to Q, U mixing) and the beam's differential eccentricity must be well controlled. To prevent conversion of the E-mode signal into B-mode signals the residual instrumental cross-polarization (Stokes's Q to U rotation) after calibration must be below -50 dB. In order to characterize and subtract these systematic effects, a number of modulation schemes are required.

B. Overall instrument design

The two Clover instruments are polarimetric imaging arrays on dedicated telescopes and mounts, with a 96 pixel focal plane array centered at 97 GHz on one telescope (the Low Frequency Instrument) and a mixed focal plane array of 96 pixels centered at each of 150 and 225 GHz on the second telescope (the High Frequency Instrument). The chosen frequency bands are given in Table II.

Each telescope is a $\sim 1.5 - 1.8$ m compact range antenna (CRA) on an alt-az mount with an additional axis allowing rotation of the whole instrument about the pointing direction

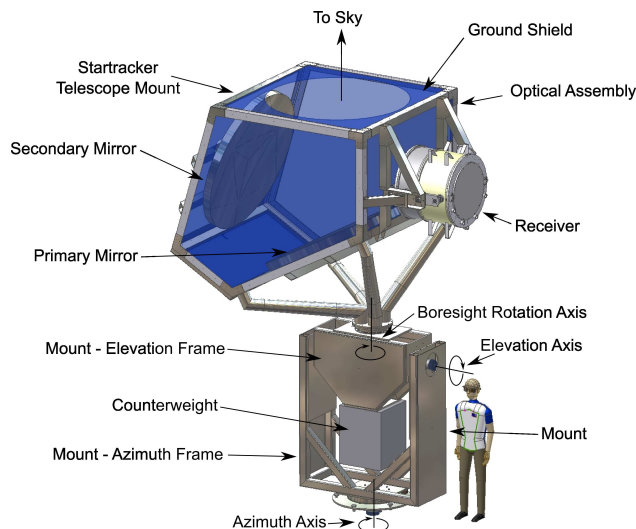


Figure 1. CAD drawing of one of the two Clover instruments. The receiver is on the left, with the absorbing ground screen surrounding the optics shown in blue.

of the telescope. The optics are designed to give extremely low sidelobes (below 1.6% spillover power) and very low cross-polarization across a large, flat focal plane [7]. In order to reduce the effect of polarized sidelobes from the instrument, the receiver and optics are surrounded by co-mounted absorbing ground screens that provide a constant background load for all sidelobes. An artist's impression of one of the two Clover instruments is shown in fig. 1.

All the pixels consist of profiled corrugated horns, feeding turnstile waveguide OMTs [8] in the low frequency instrument (LF), and circular waveguide probe OMTs [9] integrated into the detector chips in the 150 and 225 GHz pixels in the high frequency instrument (HF). The outputs of the OMTs are used to feed microstrip coupled molybdenum-copper transition edge sensor bolometers [10], via finline-to-microstrip transitions [11] in the low frequency instrument, and directly from the waveguide probes in the high frequency instrument. The bolometers are read using time division multiplexed (TDM) SQUID amplifiers developed by NIST and room temperature multi-channel electronic (MCE) systems developed by University of British Columbia [12], [13].

During CMB observations, the primary modulation of the sky signal is provided by rapidly scanning the instruments across the sky at a constant elevation, to provide a constant atmospheric power contribution, while the sky field drifts through the scanning elevation. The telescopes and mounts have been designed for scanning speeds up to $10^\circ/\text{s}$ across a 20° diameter field, although slower scan speeds are likely to be preferred, to provide separation between the pixel crossing rate and polarization modulation rate, and to reduce the observing time overheads associated with turning the telescopes around at the end of each scan [14].

Polarization modulation is provided by two methods; firstly a rotating metal mesh half-wave plate is used to provide rapid polarization modulation at the input to the focal plane arrays. This half-wave plate may be operated either in a continuously rotating mode, or with a stepped rotation between scans.

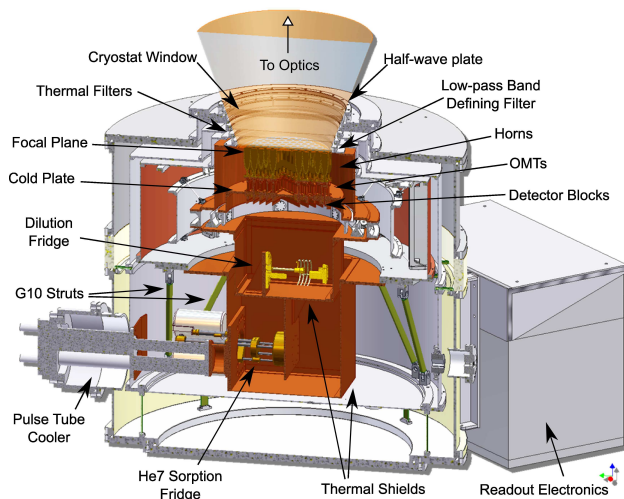


Figure 2. Cross-section through the LF instrument receiver. From the top, the signal from the telescope passes through the AHWP, cryostat window and filter stack. The focal plane array of horns and OMTs are positioned just behind the filter stack, with the blocks of 16 detectors mounted on the other side of the 100 mK cold plate. The detectors are readout by a TDM SQUID readout system mounted on the 4 K stage, which is in turn read by the multi-channel electronics mounted on the right hand side. The cold plate is cooled by the miniature dilution fridge at the centre of the receiver, which is in turn cooled by the He7 sorption fridge and pulse tube cooler at the lower left.

Additionally, the entire instrument, including the optics, can be rotated about the pointing direction. This modulation is slow, and so is likely to be used between sets of several scans, or between observing sessions [15].

C. Optics

The Clover optics design is based on the compact range antenna design described in [7]. This design of antenna has been shown to give excellent cross-polarization performance across a large flat focal plane, allowing a large number of detectors to be fed directly without requiring additional focusing optics that may introduce chromatic aberrations or cross-polarization, or the complexity of a curved focal plane.

The key parameters of the design of the optics for the two instruments are given in table III. The performance of both optical systems has been extensively simulated using the GRASP physical optics package to minimize the cross-polarization and spillover performance while retaining the large focal plane areas. A summary of the optical performance results is given in table IV.

In order to prevent a 300 K background seen by spillover sidelobes from overloading the TES bolometers, the total power in the sidelobes has to be kept below 1.6%. The residual far out sidelobes are terminated on a co-mounted absorbing ground shield to provide a stable polarization signal background when the telescope is pointed in different directions. The calculated spillover pattern for a pixel at the edge of the focal plane on the LF instrument is shown in fig. 4.

Each of the Clover mirrors was CNC machined from a single piece of aluminum. The back of the mirror is light-weighted by machining away most of the backing material, leaving a number of ribs to provide structural strength and

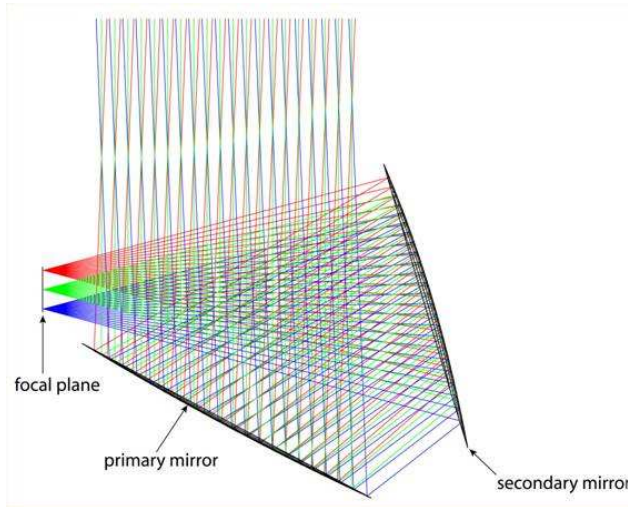


Figure 3. Schematic of the Clover CRA optics. Light from the sky is reflected from the parabolic primary mirror to the concave hyperboloidal secondary mirror before being focused on the focal plane, positioned perpendicular to the incoming wavefront from the sky.

Table III
PARAMETERS OF THE CLOVER OPTICS

Parameter	97 GHz	150, 225 GHz
Projected aperture	1.80 m	1.50 m
Effective focal length	2961 mm	2700 mm
F/#	1.64	1.80
Primary/secondary angle	65°	65°
Feed/secondary angle	25°	25°
Primary focal length	6350 mm	5790 mm
Primary offset	-6778 mm	-6180 mm
Secondary foci distance	8740 mm	7950 mm
Secondary vertex distance	-4227 mm	-3845 mm
Secondary eccentricity	-2.0674419	-2.0674419
Feed FWHM	14.5°	14.4°, 9.4°

Table IV
PERFORMANCE OF THE CLOVER OPTICS. IN EACH CASE, THE BEST AND WORST PERFORMING PIXEL IS SHOWN

Parameter	97 GHz	150 GHz	225 GHz
Beamwidth	7.5', 7.7'	5.46', 5.55'	5.28', 5.34'
Beam eccentricity	0.11, 0.21	0.14, 0.27	0.11, 0.19
Cross-polarization	-39, -38 dB	-43, -41 dB	-45, -42 dB
First sidelobes	-35, -22 dB	-31, -19 dB	-44, -26 dB
Far-out sidelobes	< -70 dB	< -70 dB	-
Spillover	1.26, 1.62%	1.85, 2.60%	0.08%, 0.27%

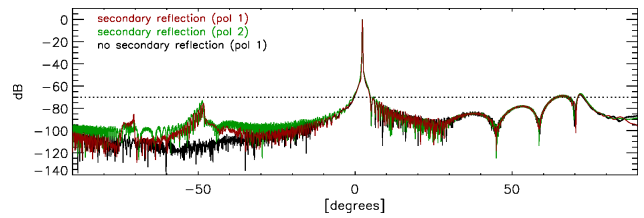


Figure 4. Far out sidelobe pattern calculated by GRASP for an edge pixel on the Clover LF instrument.

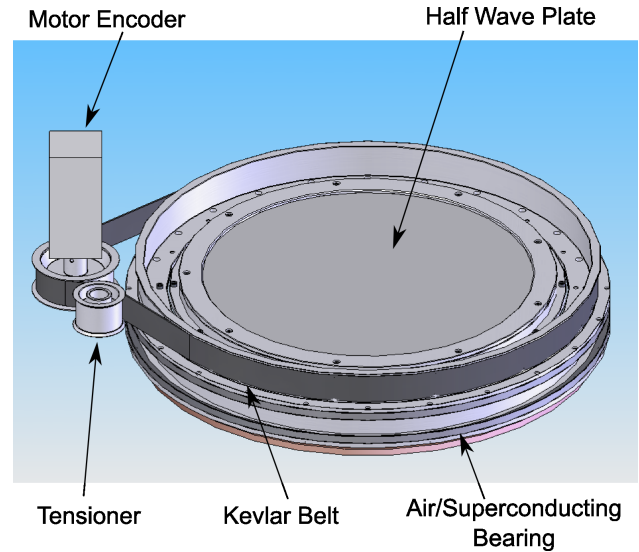


Figure 5. CAD model of the HF instrument achromatic half-wave plate on its superconducting magnetic levitation bearing and with the Kevlar belt and motor used to drive the AHWP.

location for three adjustable mounting points per mirror. The optical assembly skin is lined with Eccosorb HR-10 open cell foam absorber, with a closed cell polythene foam covering the Eccosorb HR-10 to provide weather protection for the absorber. The reflectivity of this absorber system has been measured as less than 3% at 150 GHz [16].

D. Half-wave plate, vacuum window and filter stack

Polarization modulation is applied to each array by an achromatic half-wave plate (AHWP) placed in front of each focal plane. Each AHWP is of hot-pressed metal mesh on plastic design of similar construction to the thermal and low-pass filters. By stacking alternate layers of capacitive and inductive grid patterns, phase differences of 180° can be achieved between orthogonal polarizations across large bandwidths.

The Clover LF AHWP operates over a 30% bandwidth centered at 97 GHz, and is mounted just in front of the cryostat window in a dry air flushed chamber. The AHWP runs on a large air bearing and is driven by a motor/encoder system via a Kevlar belt. This system provides accurate position control of the AHWP both in motion and when held in one place.

The HF AHWP has to cover two 30% wide bands, centered at 150 GHz and 225 GHz simultaneously. This means that considerably more layers are required to produce the AHWP, and so to reduce the absorption loss, the HF AHWP is placed

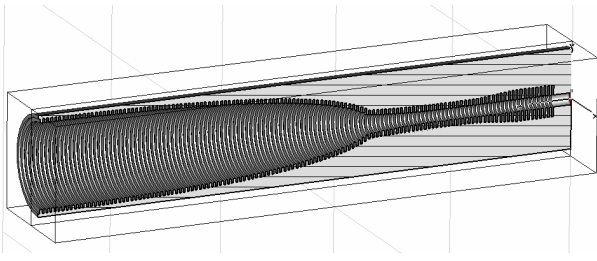


Figure 6. The profiled corrugated horn design for the Clover LF instrument.

just inside the cryostat window and thermally anchored to the 60 K radiation shield stage. The HF AHWP rotates on a superconducting magnetic levitation bearing, and is driven by a motor and Kevlar belt as on the LF instrument system (Fig. 5).

The window of each cryostat is made of ultra-high molecular weight polythene with a very low absorption coefficient. To withstand the 1 bar pressure difference over the 300 mm window diameter, the window needs to be 8 mm thick. Anti-reflection coatings of porous PTFE are used to reduce the Fabry-Perot fringing due to the thick dielectric.

The thermal load on the cold stage of the cryostat is reduced by using a number of reflective metal mesh low-pass filters with low emissivity near the observing bands. Since these dielectric material used to support the metal mesh becomes opaque in the mid-infrared, a number of low pass thermal filters are required, mounted on various thermal shields to gradually reduce the emission towards the cold-stage.

In the LF instrument, the upper edge of the observing band is defined by a multistage metal mesh filter placed across the whole focal plane. The low edge of the band is defined by a constriction in the throats of the horns. The mixed frequency nature of the HF focal plane means that individual low-pass filters are required on each horn to define the upper edge of the band individually for each pixel.

E. Feed horns and focal plane arrays

All the feed-horns are individually electroformed profiled corrugated horns with a high-pass corrugated waveguide filter at the throat to define the lower edge of the observation band (Fig. 6). The measured beam pattern for a 97 GHz horn is shown in fig. 7.

In the LF instrument, the detectors are gathered in linear blocks of 16, fed by eight horns and OMTs, and arranged as shown in fig. 8. Each detector block contains a single time-domain SQUID multiplexer chip that reads all 16 detectors.

In the HF instrument, the detectors and horns are gathered in 2×4 blocks, with one row of four offset from the other to allow for close hexagonal packing. The detector blocks are arranged as shown in fig. 8, with the 150 GHz detectors at the centre of the array, and the 225 GHz pixels at the edge of the array. Due to the strong under-illumination of the optics by the 225 GHz horns, placing the 225 GHz pixels at the edge of the focal plane does not significantly degrade the optical performance for these detectors.

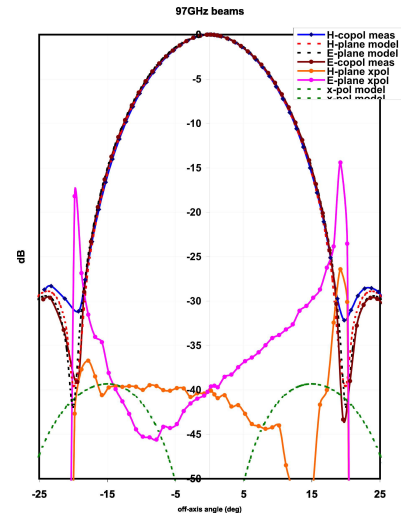


Figure 7. Measured beam pattern for a Clover LF horn. The cross-polarization measurement is limited by the accuracy of alignment between the transmitter and receiver horns.

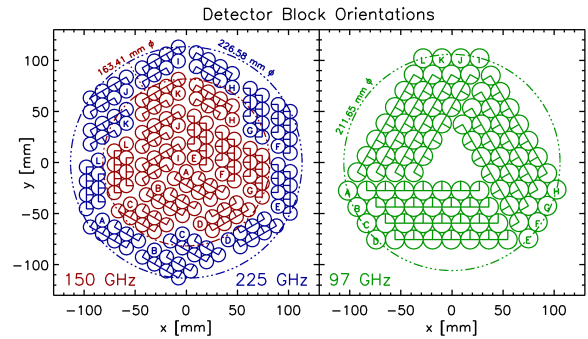


Figure 8. Layout of the two focal plane arrays. The H-plane polarization direction is shown by the short half-line on each circle. The dashed circles show the radius from the center of the array to the centre of the outermost pixel at each frequency.

F. OMTs

The low frequency instrument uses individual electroformed waveguide OMTs to separate the polarization components. The OMT is a turnstile design (fig. 9) fed by the circular waveguide from the feed-horn, and with tapered Y-junction waveguide power combiners that include a 90° twist in one arm to provide parallel waveguides at the outputs to the detector block [8]. Measured performance of the OMTs is shown in fig. 10.

The high frequency instrument uses four rectangular probes integrated onto the detector chip [9], [10] to both split the polarization components and to feed the TES detectors (figs. 11 and 12). The four rectangular probes are fabricated in niobium on a silicon nitride membrane that is mounted across the circular waveguide in front of a fixed back-short. The silicon nitride membrane is extended $\lambda/4$ into the waveguide walls in a narrow gap formed by extending the lower half of the circular waveguide walls into the well in the silicon detector chip that supports the membrane. The probes feed the microstrip inputs to the TES absorbers across a grounding ring that sits just above the end of the circular waveguide and capacitively couples to the edges of the gap in the waveguide. The signal

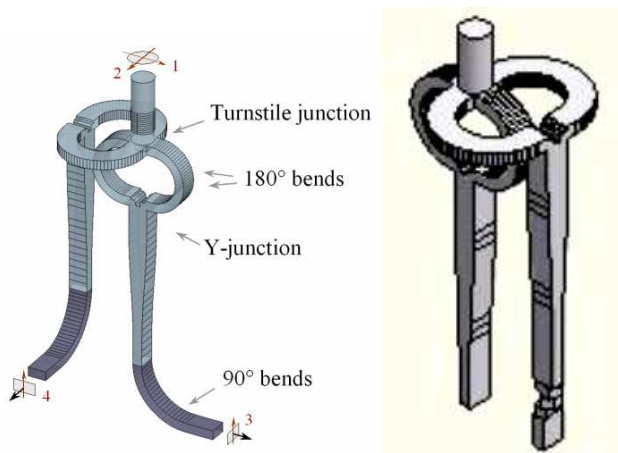


Figure 9. The prototype LF OMT (left) and the final design incorporating the waveguide twist required to bring both polarization components out in parallel waveguides.

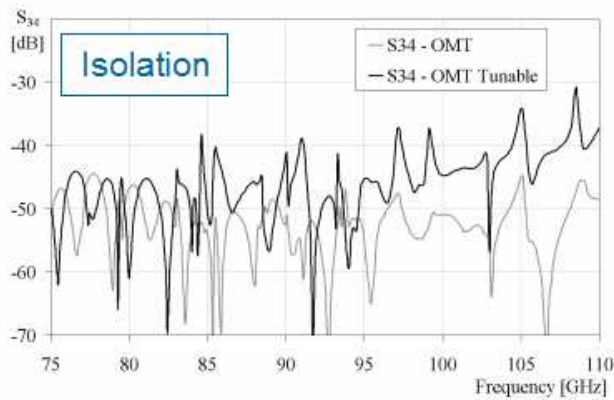


Figure 10. Measured polarization isolation (cross-polarization) for the LF prototype OMT and for an alternative prototype with a tunable turnstile stub.

from each polarization component is split 50:50 between the two probes on opposite sides of the OMT. These signals are recombined incoherently on the TES islands.

G. Detectors

In the low frequency instrument, the TES bolometers are fed from the waveguide OMTs via unilateral finline waveguide-to-microstrip transitions on the 225 μm thick silicon detector substrate [10], [17]. The design of the finline transition is described in [11]. To prevent the excitation of higher order modes in the finline, the WR-10 waveguide is reduced in height from 1.27 mm to 1.1 mm, and the finline has serrations placed in the support slots at either side of the chip. The finline detectors are mounted in a copper E-plane split waveguide block that houses 16 detectors, as well as the TDM readout chips.

In the high frequency instrument, the output of the rectangular probes on silicon nitride membrane are coupled to three section quarter-wave transformers, implemented in microstrip, to match the 50 Ω probe output to the 23 Ω microstrip line that feed the TES bolometers [10]. The two probes that couple to each polarization component are connected to two

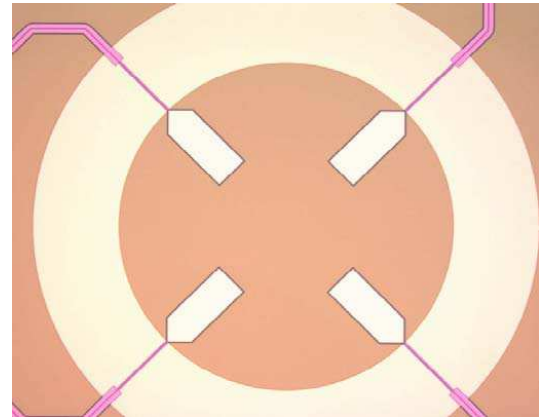


Figure 11. The HF microstrip coupled probe OMT, showing the probes, grounding ring, silicon nitride membrane and output microstrips. The circular waveguide output from the horn is aligned with the inner edge of the niobium grounding ring (yellow) and a quarter wave back-short waveguide is built into the detector block (see fig. 15).

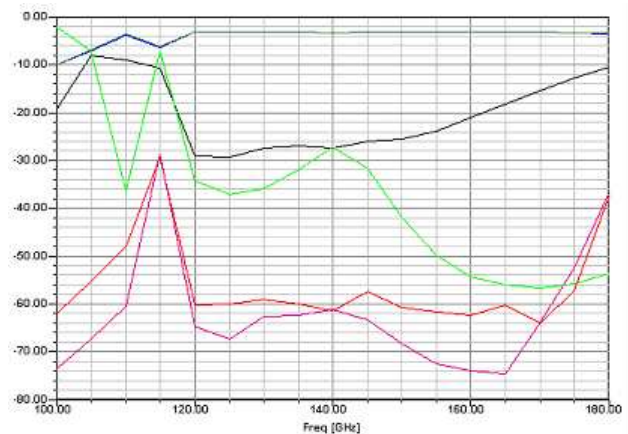


Figure 12. Results of HFSS simulations of the 150 GHz probe OMT, including the microstrip transformer.

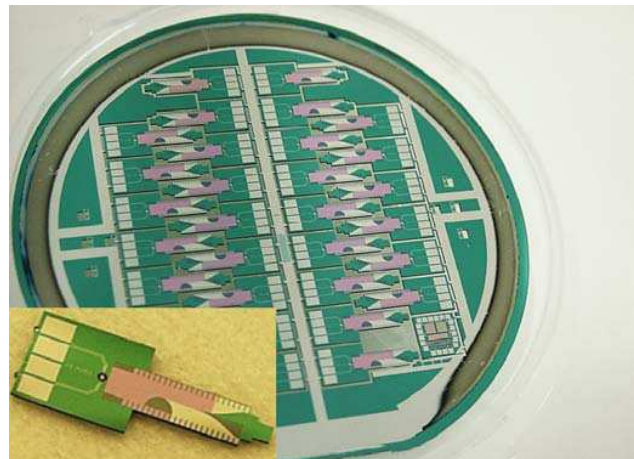


Figure 13. The 97 GHz second generation detectors.

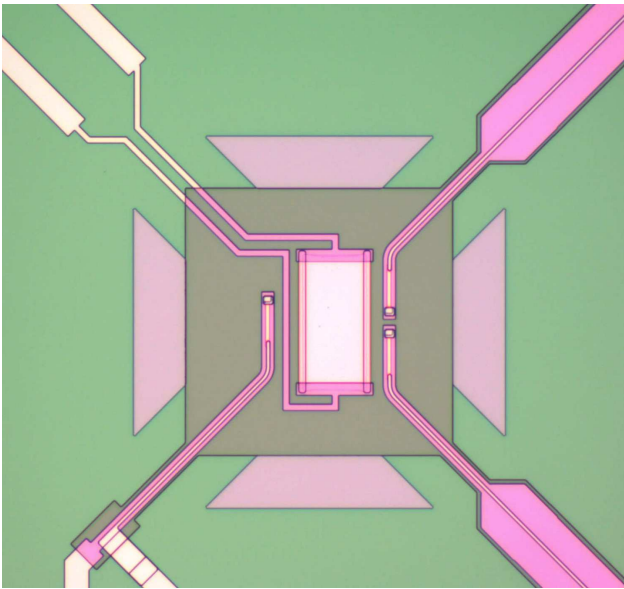


Figure 14. The HF detector's TES island, with two microstrip inputs from the two probes at the bottom, the TES bias wiring at the top left and the heater wiring at the top right.



Figure 15. A prototype HF detector mounted in the detector module block. Bias signals and heater power are taken from the two TES detectors on superconducting pins through the block to the readout system on the back of the focal plane array. The circular waveguide back-short is visible through the centre of the detector chip.

resistors on a single TES island, so that the power is combined incoherently (fig. 14).

In both instruments, the niobium microstrip transmission lines carry the signal along one of the silicon nitride legs onto islands where the signal is converted to heat in a termination resistor made of gold/copper alloy. The termination resistor is matched to input microstrip line impedance, giving a return loss better than -25 dB.

The input signal is detected by molybdenum/copper proximity effect bi-layer transition edge sensors with a transition temperatures of 190 mK for the 97 GHz and 150 GHz detectors and 430 mK for the 225 GHz detectors. The TES are fabricated on islands suspended on four $0.5 \mu\text{m}$ thick silicon

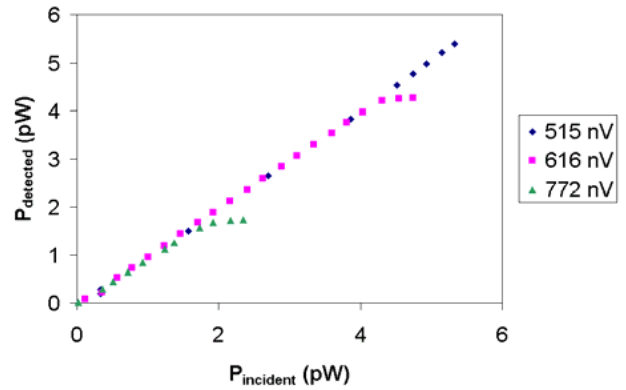


Figure 16. Detected power versus incident power at a variety of bias voltages for the prototype 97 GHz finline TES detectors [17].

nitride legs for thermal isolation. The input RF signal is carried on microstrip down one or two legs, while the TES readout leads run down one of the other legs. The fourth leg is used to carry DC power to a resistor, matched to the RF termination resistor for calibration purposes and to keep the received power on the TES constant in the presence of a changing power load from the sky. Interdigitated copper fingers are used to suppress excess noise in the TES due to internal thermal fluctuation noise by improving the thermalisation across the TES.

The detectors are fabricated on $225 \mu\text{m}$ silicon substrates with $0.5 \mu\text{m}$ low stress silicon nitride membrane. The Mo/Cu TES, copper fingers and banks are deposited first, followed by the niobium transmission line ground plane and TES contact leads, silicon dioxide insulation layer, Au/Cu resistors and niobium transmission line wiring layer. The detector chip is shaped by deep reactive ion etching (DRIE), which is also used to etch the well under the TES island. All detector fabrication processes apart from the DRIE are carried out by the Detector Physics Group at the Cavendish Laboratory [18].

Prototypes have been fabricated for both the low and high frequency detectors, and production of the science grade 97 GHz detectors is complete. Dark NEPs have been measured at $\sim 1.7 \times 10^{-17} \text{ W}/\sqrt{\text{Hz}}$ with time constants $\tau \sim 10^{-4} \text{ s}$ for the 97 GHz detector design [17], comfortably within the performance requirements for Clover. Optical tests have been carried out at 97 GHz, using a temperature controlled blackbody load within the test cryostat. These indicate that the optical efficiencies of the science grade 97 GHz detectors are better than 70%.

H. Readout

In order to reduce the heat load on the cold stage of the cryostat, the TES detectors are read by a time division multiplexing system supplied by NIST [12]. This significantly reduces the number of wires required between the cold stage and room temperature. Each TES is operated in a flux locked loop to its own first stage SQUID. These SQUIDs are addressed in sequence to provide multiplexing and the current is amplified by an on-chip second-stage SQUID and then by a separate SQUID series array. Each NIST SQUID multiplexing chip is capable of reading up to 32 TES, with one additional

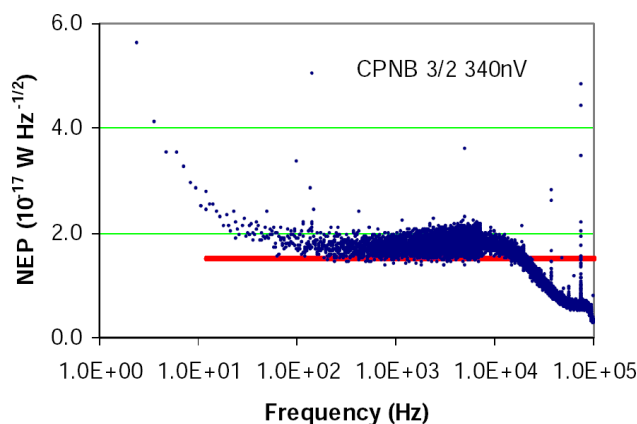


Figure 17. Measured noise spectrum for a prototype 97 GHz finline TES detector [17].

dark channel. In Clover, only 16 TES will be connected to each multiplexing chip due to packaging constraints. However, this scheme has the important advantages of reduced aliasing noise and allowing the selection of the most similar first stage SQUIDs on each chip and bypassing failed channels. The output of the SQUID TDM system is read by room temperature multichannel electronics supplied by University of British Columbia [13].

I. Cryogenics and magnetic shielding

Both Clover's focal plane arrays are cooled in closed-cycle three-stage cryostats. A CryoMech PT410 pulse tube cooler, modified for lower vibration operation, provides of 1 W of cooling power at 4 K, as well as the 50 K stage used to cool the radiation shields (and AHWP in the HF instrument). A closed cycle "He-7" $^3\text{He}/^4\text{He}$ sorption fridge is mounted on the 4 K stage, providing $400 \mu\text{W}$ at 400 mK. On the 400 mK stage a closed cycle miniature dilution refrigerator [19] is used to provide $3 \mu\text{W}$ of cooling power at 100 mK to the TES detectors. The temperature of the 100 mK stage is actively controlled to provide a temperature stability of $60 \text{ nK}/\sqrt{\text{Hz}}$ at 100 mK, with a long-term variation of $< 3.5 \mu\text{K}$ over a 24 hour duty cycle. Additional temperature stages at 3 K, 1.1 K and 700 mK are available for heatsinking various components of the sorption and dilution fridges, gas gap heat switches and cables.

A major difficulty with the cryogenics has been the requirement that the cryostat must be tipped as the telescopes point around the sky. By carefully choosing the mounting angles of the cryocoolers and limiting the range of allowed boresight and elevation angles, then the angle of the cryocoolers can be kept to within 45° from the vertical, while pointing the telescope up to 60° from the zenith with an adequate range of boresight angles to allow polarization systematics to be detected. This requirement has necessitated the development of novel designs of He-7 sorption coolers and miniature dilution refrigerators. At specific boresight angles, the telescopes can point to the horizon, allowing sky dips and other calibration observations to be made.

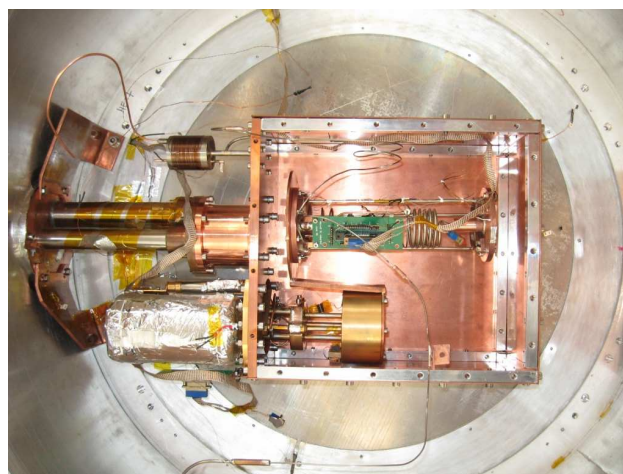


Figure 18. Pulse tube cooler head (left), 4 K box, He-7 sorption fridge (centre bottom) and prototype dilution fridge (centre) installed in the Clover LF cryostat.

J. Telescope mounts

Each of the two Clover instruments has its own three-axis mount. Both mounts are alt-az mounts with an additional bore-sight rotation axis used to rotate the whole telescope about its pointing direction to allow for the calibration of instrumental polarization. Each axis is driven by an extremely compact Harmonic Drive motor/encoder assembly. The mounts are able to maintain a pointing accuracy of $20''$, with a long-term tracking accuracy of $60''$, while being able to carry out constant elevation scans at speeds of up to 10 deg/s with turn-around accelerations up to 20 deg/s^2 .

Each mount has an optical pointing telescope mounted on the optical assembly behind the secondary mirror, for pointing calibration during commissioning and observations. These telescopes are based on the commercial photographic lens and CCD design used on the BLAST balloon-borne telescope [20], with a change of lens and CCD to accommodate Clover's resolution and field of view.

K. Site

Clover will be sited at Pampa la Bola, on the edge of the ALMA site in the Atacama desert near San Pedro de Atacama, Chile. This 4800 m altitude site provides excellent atmospheric transparency and stability at millimeter wavelengths, as well as the possibility of sharing some infrastructure with a number of other instruments and observatories on the site.

The latitude of the site (23° S) means that a good proportion of the sky is observable at relatively high elevations, and thus low air-mass. This allows observing fields to be selected that have very low levels of foreground contamination, and that overlap with surveys undertaken by other CMB instruments.

III. OBSERVATIONS AND DATA ANALYSIS

A. Observing fields, modes and calibration

Contamination from Galactic foregrounds is a major issue for deep polarization observations of the CMB. In order to maximize the observing efficiency for Clover, the required

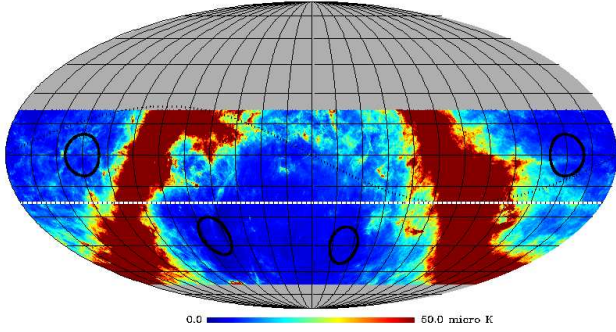


Figure 19. Clover observing fields, chosen to give year-round night time observing in regions of very low foreground contamination.

1000 deg² survey area is split into four convex fields, spread roughly evenly in right ascension, with the declination and exact right ascensions chosen to place the fields in the area of minimum foreground contamination, estimated from all-sky CMB observations and Galactic polarization surveys. The optimized Clover survey fields are shown in fig. 19.

To reduce contamination from changing sky brightness and atmospheric fluctuations, Clover will perform fast, constant elevation scans over each field as it rises and falls each night. The observations will continue for two years, giving ~ 0.8 years integration time required to achieve the required map sensitivity.

The calibration of CMB polarization experiments is challenging, as there are few well-characterized stable polarized astronomical sources at mm wavelengths. Possible calibration sources are extra-galactic radio sources such as Tau A, or planets (although planets are not highly polarized). An absolute intensity calibration uncertainty of 5% should be possible from WMAP and Planck data. For polarization calibration it may be necessary to calibrate off unpolarized sources, using a weak wire grid polarizer across the cryostat aperture. It may also be possible to use artificial sources for characterizing subtle systematic effects, either in the laboratory or in the field.

B. Data analysis

The analysis of the Clover data will be difficult, mainly due to the large amounts of data expected (~ 100 TB for a 2-year campaign). After some minimal processing of the raw time-ordered data, maps of the T, Q and U Stokes parameters (fig.20) will be constructed using a combination of naive and near-optimal (but computationally efficient) destriping techniques [21].

In order to estimate the E- and B-mode power spectra from these maps, we will adopt a Monte-Carlo based "pseudo- C_l " approach, augmented by an optimal maximum-likelihood analysis for the largest angular scales. In general, such an approach requires detailed simulations of the experiment to quantify uncertainties, correct for noise and any filtering applied to the data, and to test for systematic contaminants. We have already used our initial simulation and analysis pipeline to investigate a number of possible instrumental systematic

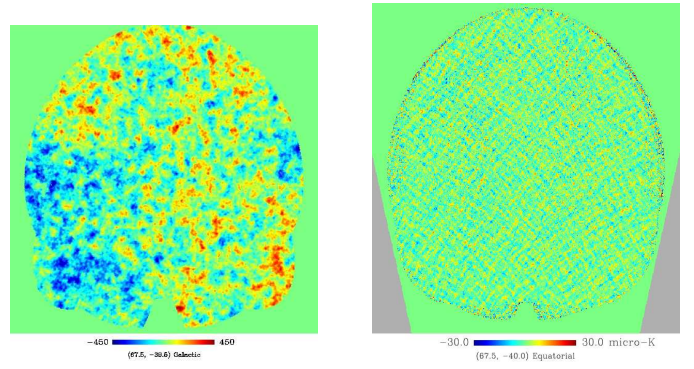


Figure 20. Sample Stokes' I (temperature) and U (polarization) maps recovered from simulated Clover observations by destriping.

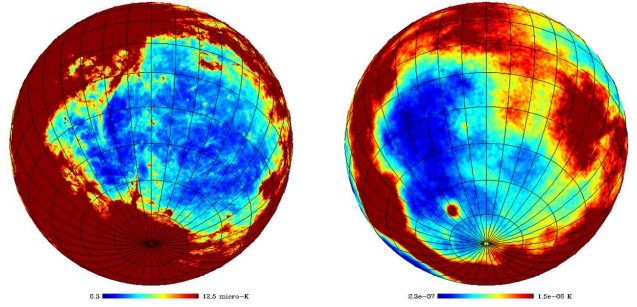


Figure 21. Template maps for foregrounds for synchrotron (left) and dust (right) contamination of the CMB sky.

effects [15] and are currently using it to assess the performance of a number of alternate foreground removal techniques.

Detecting B-mode polarization will require the removal of foreground signals, particularly those from Galactic synchrotron and dust emission, as well as other, weaker foreground signals such as anomalous spinning dust. The spectral coverage of Clover means that some degree of component separation and removal will be possible, although removing more than two bright foreground components will require additional data or modeling of the foregrounds from other experiments.

IV. PERFORMANCE PREDICTIONS AND TIMESCALE

A. Performance predictions

After 0.8 years of integration time, Clover will have mapped ~ 1000 deg² of the lowest foreground emission areas of the sky to a sensitivity of $1.7 \mu\text{K}$ per $8'$ pixel at 97, 150 and 225 GHz. It is expected that signals due to systematic effects will result in a bias in the measured tensor-to-scalar ratio of < 0.001 . The expected angular power spectra and error bars for Clover are shown in fig.22, for the current concordance Λ CDM cosmological model and tensor-to-scalar ratios $r = 0.1$ and $r = 0.026$, as well as the expected levels of foreground signals. The sensitivity and systematic effect estimates here are based on the current Clover performance requirements, given above. Detection of the primordial B-mode signal will determine the energy scale of inflation, while a non-detection of the B-mode signal at tensor-to-scalar ratio

$r > 0.026$ will provide an upper limit on the energy scale of less than $\sim 2 \times 10^{16}$ GeV.

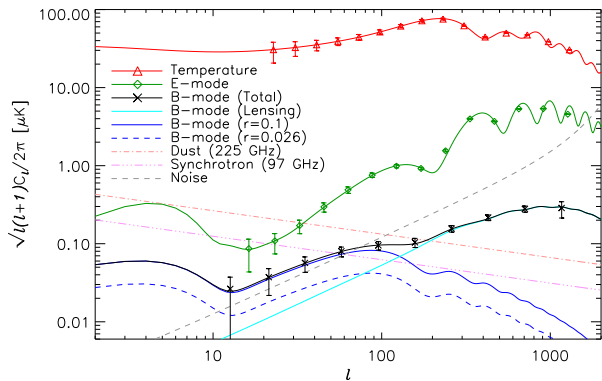


Figure 22. Predicted power spectra for Clover after 0.8 years integration time, as well as the expected instrumental noise and foreground levels before subtraction.

B. Progress and timescale

Both Clover instruments are currently in the component integration phase, with the telescopes and mounts being assembled and tested in Oxford, the cryostat, cryogenic systems and quasi-optical components (AHWPs, windows and filters) being assembled and tested in Cardiff and LF feed-horns and OMTs undergoing testing in Manchester. The production and testing of science grade LF finline detector modules and testing of the TDM readout is ongoing in Cambridge, in parallel with the final prototyping of the HF probe OMT detectors.

Assembly, integration and testing of the receivers and entire LF instrument is planned during mid to late 2009 in Cardiff and Oxford respectively, before shipping to the Clover site in Chile in early 2010 for commissioning. The HF instrument is due to follow a few months behind the LF instrument. Work on setting up the Clover site infrastructure in Chile is due to start in the next few months.

REFERENCES

[1] A. Challinor, "Constraining fundamental physics with the cosmic microwave background," *ArXiv e-print*, vol. astro-ph/0606548, 2006.
 [2] W. Hu and M. White, "A CMB polarisation primer," *New Astronomy*, vol. 2, no. 323, 1997.
 [3] D. O'Dea, A. Challinor, and B. R. Johnson, "Systematic errors in cosmic microwave background polarization measurements," *MNRAS*, vol. 376, no. 4, p. 1767, 2007.
 [4] D. P. Finkbeiner, M. Davis, and D. J. Schlegel, "Extrapolation of Galactic Dust Emission at 100 microns to Cosmic Microwave Background Radiation Frequencies using FIRAS," *ApJ*, vol. 524, p. 867, 1999.
 [5] G. Giardino, A. J. Banday, K. M. Górski, K. Bennett, J. L. Jonas, and J. Tauber, "Towards a Model of Full-sky Galactic Synchrotron Intensity and Linear Polarisation: A re-analysis of the Parkes data," *A&A*, vol. 387, p. 82, 2002.
 [6] A. Otárola, M. Holdaway, L.-E. Nyman, S. Radford, and B. Butler, "Atmospheric transparency at Chajnantor: 1973-2003," *ALMA Memo Series*, vol. 512, 2005.
 [7] G. Yassin, P. K. Grimes, and S. B. Sorenson, "Compact optical assemblies for large-format imaging arrays," in *Proceedings of the 16th Int. Symp. on Space THz Tech.*, (Gothenburg, Sweden), 2005.

[8] G. Pisano, L. Pietranera, K. Isaak, L. Piccirillo, B. Johnson, B. Maffei, and S. Melhuish, "A Broadband WR10 Turnstile Junction Orthomode Transducer," *IEEE Microwave Compon. Lett.*, vol. 17, no. 4, p. 286, 2007.
 [9] P. K. Grimes, O. G. King, G. Yassin, and M. E. Jones, "Compact broadband planar orthomode transducer," *Electronic Letters*, vol. 43, no. 21, p. 1146, 2007.
 [10] M. D. Audley, D. M. Glowacka, D. J. Goldie, V. N. Tsaneva, S. Withington, P. K. Grimes, C. E. North, G. Yassin, L. Piccirillo, G. Pisano, P. A. R. Ade, P. Mauskopf, R. V. Sudiwala, J. Zhang, K. D. Irwin, M. Halpern, and E. Battistelli, "Microstrip-coupled TES bolometers for CLOVER," in *Proceedings of the 19th Int. Symp. on Space THz Tech.*, (Groningen), Apr. 2008.
 [11] G. Yassin, P. K. Grimes, O. G. King, and C. E. North, "Waveguide-to-planar circuit transition for millimetre-wave detectors," *Electronic Letters*, vol. 44, no. 14, 2008.
 [12] C. D. Reintsema, J. Beyer, S. W. Nam, S. Deiker, G. C. Hilton, K. D. Irwin, J. Martinis, J. Ullom, and L. R. Vale, "Prototype system for superconducting quantum interference device multiplexing of large-format transition-edge sensor arrays," *Rev. Sci. Instrum.*, vol. 74, no. 10, p. 4500, 2003.
 [13] E. S. Battistelli, M. Amiri, B. Burger, M. Halpern, S. Knotek, M. Ellis, X. Gao, D. Kelly, M. Macintosh, K. Irwin, and C. Reintsema, "Functional Description of Read-out Electronics for Time-Domain Multiplexed Bolometers for Millimeter and Sub-millimeter Astronomy," *J. Low Temp. Phys.*, vol. 151, p. 908, May 2008.
 [14] C. E. North, B. R. Johnson, P. A. R. Ade, M. D. Audley, C. Baines, R. A. Battye, M. L. Brown, P. Cabella, P. G. Calisse, A. D. Challinor, W. D. Duncan, P. G. Ferreira, W. K. Gear, D. Glowacka, D. J. Goldie, P. K. Grimes, M. Halpern, V. Haynes, G. C. Hilton, K. D. Irwin, M. E. Jones, A. N. Lasenby, P. J. Leahy, J. Leech, B. Maffei, P. Mauskopf, S. J. Melhuish, D. O'Dea, S. M. Parsley, L. Piccirillo, G. Pisano, C. D. Reintsema, G. Savini, R. Sudiwala, D. Sutton, A. C. Taylor, G. Teleberg, D. Titterton, V. Tsaneva, C. Tucker, R. Watson, S. Withington, G. Yassin, and J. Zhang, "Detecting the B-mode Polarisation of the CMB with Clover," *ArXiv e-prints*, vol. astro-ph/0805.3690, May 2008.
 [15] M. L. Brown, A. Challinor, C. E. North, B. R. Johnson, D. O'Dea, and D. Sutton, "Impact of modulation on CMB B-mode polarization experiments," *ArXiv e-print*, vol. astro-ph/0809.4032.
 [16] K. W. Yoon, P. A. R. Ade, D. Barkats, J. O. Battle, E. M. Bierman, J. J. Bock, J. A. Brevik, H. C. Chiang, A. Crites, C. D. Dowell, L. Duband, G. S. Griffin, E. F. Hivon, W. L. Holzapfel, V. V. Hristov, B. G. Keating, J. M. Kovac, C. L. Kuo, A. E. Lange, E. M. Leitch, P. V. Mason, H. T. Nguyen, N. Ponthieu, Y. D. Takahashi, T. Renbarger, L. C. Weintraub, and D. Woolsey, "The Robinson Gravitational Wave Background Telescope (BICEP): a bolometric large angular scale CMB polarimeter," *Proceedings of the SPIE*, vol. 6275, July 2006.
 [17] M. D. Audley, D. M. Glowacka, D. J. Goldie, V. N. Tsaneva, S. Withington, P. K. Grimes, C. E. North, G. Yassin, L. Piccirillo, P. A. R. Ade, and R. V. Sudiwala, "Performance of microstrip-coupled TES bolometers with finline transitions," *Proceedings of the SPIE*, vol. 7020, p. 70200G, 2008.
 [18] D. Glowacka, D. Goldie, S. Withington, M. Crane, V. Tsaneva, M. Audley, and A. Bunting, "A fabrication process for microstrip-coupled superconducting transition edge sensors giving highly reproducible device characteristics," *J. Low Temp. Phys.*, vol. 151, p. 249.
 [19] G. Teleberg, S. T. Chase, and L. Piccirillo, "A Cryogen-Free Miniature Dilution Refrigerator for Low-Temperature Detector Applications," *J. Low Temp. Phys.*, vol. 151, no. 3-4, p. 669, 2008.
 [20] E. Pascale, P. A. R. Ade, J. J. Bock, E. L. Chapin, J. Chung, M. J. Devlin, S. Dicker, M. Griffin, J. O. Gundersen, M. Halpern, P. C. Hargrave, D. H. Hughes, J. Klein, C. J. MacTavish, G. Marsden, P. G. Martin, T. G. Martin, P. Mauskopf, C. B. Netterfield, L. Olmi, G. Patanchon, M. Rex, D. Scott, C. Semisch, N. Thomas, M. D. P. Truch, C. Tucker, G. S. Tucker, M. P. Viero, and D. V. Wiebe, "The Balloon-borne Large Aperture Submillimeter Telescope: BLAST," *ApJ*, vol. 681, pp. 400-414, July 2008.
 [21] D. Sutton, B. R. Johnson, M. L. Brown, P. Cabella, P. G. Ferreira, and K. M. Smith, "Map making in small field modulated CMB polarization experiments: approximating the maximum likelihood method," *MNRAS*.